Cooling and rotational dynamics of compact stars

Armen Sedrakian

ITP, Goethe-Universität, Frankfurt am Main

Compact Stars in the QCD Phase diagram/ WG2 Meeting of COST

L'Aquila, Italy, 26 May 2016

Plan of this talk

1. Pair-breaking emission processes on neutrinos and axions
2. Axion cooling of neutron stars
3. Unpairing effect in strong magnetic fields
4. Mutual friction in magnetars

Strategy for constraining axions

1. Using cooling models of light stars - no exotics - just hadron matter
2. Using benchmarked code - results are easily reproducible with standard input (we use NSCool by Dany Page)
3. Consider a small sample of neutron stars with well measured temperature and good model atomspheres
4. Only "conservative" physics is used as an input

Master equation for cooling of compact stars

$$\boxed{\left(\int_0^{R_c} nc_v(r,T)dV_p\right)\frac{dT'}{dt} = -\int_0^{R_c} n\epsilon_\nu(r,T)e^{2\Phi}dV_p - 4\pi\sigma R^2 T_S^4 e^{2\Phi_c}} \qquad (1)$$

- Urca process produce only neutrons (need a charged lepton in the final state)

$$n \to p + e + \bar{\nu}, \qquad x_p > 11\%, \quad n + n \to n + p + e + \bar{\nu}.$$

- Fermion bremsstrahlung both on neutrinos and axions above T_c

$$N + N \to N + N + \nu + \bar{\nu}, \qquad N + N \to N + N + a.$$

- Crust bremsstrahlung (latex time cooling, but not in hadronic axion models)

$$e + (A,Z) \to e + (A,Z) + \nu + \bar{\nu}, \quad e + (A,Z) \to e + (A,Z) + a. \qquad (2)$$

- Cooper-pair-breaking processes on neutrons and axions

$$\boxed{[NN] \to [NN] + \nu + \bar{\nu}, \quad [NN] \to [NN] + +a.} \qquad (3)$$

Pairing patterns in nuclear matter

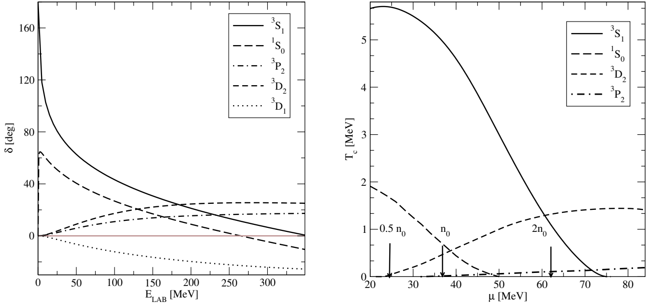

Figure : Left panel: Scattering phase shifts in different channels. Right panel: Critical temperature of superfluid phase transitions in different channels

Start with neutrinos.

Many authors considered the case of neutrinos (Kolomeitsev and Voskresensky, Leinson and Perez, Steiner and Reddy, Sedrakian et al ....)

The neutrino emissivity is expressed in terms of the polarization tensor of baryonic matter

$$\varepsilon_{\nu\bar{\nu}} = -2\left(\frac{G_F}{2\sqrt{2}}\right)^2 \int d^4q\, g(\omega)\omega \sum_{i=1,2} \int \frac{d^3 q_i}{(2\pi)^3 2\omega_i} \Im[L^{\mu\lambda}(q_i)\, \Pi_{\mu\lambda}(q)]\delta^{(4)}(q - \sum_i q_i),$$

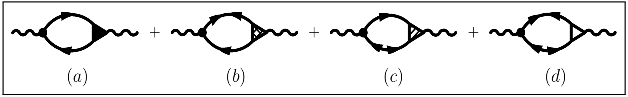

The sum of polarization tensors contributing to the vector-current neutrino emission rate. Note that the diagrams b, c, and d are specific to the superfluid systems and vanish in the unpaired state.

The result can be cast as

$$\epsilon = \frac{G^2 c_V^2 N_f}{48\pi^4} \int_0^\infty d\omega\, g(\omega)\omega J(\omega),$$

where $c_V = 1$ for neutrons and $c_V = 0.08$ for protons, $N_f = 3$ is the number of neutrino flavors in the Standard Model, and

$$J(\omega) \quad = \quad \int_0^\omega d\boldsymbol{q}\boldsymbol{q}^2(\boldsymbol{q}^2 - \omega^2)\mathrm{Im}\,[\Pi_{00}(\omega, q) - \Pi_{ii}(\omega, q)] \propto v^4 + O(v^6) \tag{4}$$

The vector current emissivity is given by ($z = \Delta/T$)

$$\epsilon = \frac{16 G^2 c_V^2 \nu(0) v_F^4}{1215\pi^3} I(z) T^7, \quad I(z) = z^7 \int_1^\infty \frac{dy\, y^5}{\sqrt{y^2-1}} f(zy)^2 \left[1 + \left(\frac{7}{33} + \frac{41}{77}\gamma\right) v_F^2\right].$$

Dependence of the integral on reduced temperature T/T_c. Higher order corrections to the leading order result are shown in lower panel.

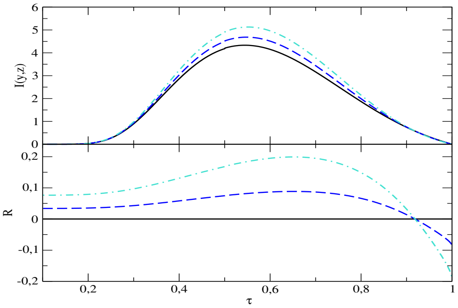

Conclusion: Vector current contribution scales as v^4 and, therefore, is suppressed.

Figure : The two diagrams contributing to the polarization tensor of baryonic matter, which defines the axial vector emissivity. The "normal" baryon propagators for particles (holes) are shown by single-arrowed lines directed from left to right (right to left). The double arrowed lines correspond to the "anomalous" propagators F (two incoming arrows) and F^+ (two outgoing arrows).

The emissivity of this processes is given by

$$\epsilon_\nu = \frac{4G_F^2 g_A^2}{15\pi^3}\zeta_A \nu(0) {v_F}^2 T^7 I_\nu, \quad I_\nu = z^7 \int_1^\infty dy \frac{y^5}{\sqrt{y^2-1}} f_F(zy)^2 . \tag{5}$$

Note the v_F^2 scaling of the axial neutrino emissivity compared to the v_F^4 scaling.
Conclusion: Axial neutrino emissivity dominates the vector current emissivity because of v^2 scaling instead of v^4 scaling.

Axion pair-breaking emissivity

Why do we need axions?

$$\mathcal{L}_{QCD} = \sum_q \bar{\psi}_q (iD - m_q e^{i\theta_q})\psi_q - \frac{1}{4} G_{\mu\nu a} G_a^{\mu\nu} - \theta \frac{\alpha_s}{8\pi} G_{\mu\nu a} \tilde{G}_a^{\mu\nu} \tag{6}$$

The phase can be pushed in the last term by chiral rotation $\psi_q' = e^{-i\gamma_5 \theta_q/2}\psi_q$

$$\mathcal{L}_{QCD} = \sum_q \bar{\psi}_q (iD - m_q)\psi_q - \frac{1}{4} G_{\mu\nu a} G_a^{\mu\nu} - \underbrace{(\theta - \arg \det M_q)}_{\bar{\theta}} \frac{\alpha_s}{8\pi} G_{\mu\nu a} \tilde{G}_a^{\mu\nu} \tag{7}$$

Experimental value: $\bar{\theta} \leq 10^{-11}$ comes from neutron electric dipole moment

$$|d| = 0.63 \times 10^{-25}\, e\, cm \tag{8}$$

Strong CP Problem: Why $\bar{\theta}$ is so small? The idea is to re-interpret the $\bar{\theta}$ term as a dynamical field

$$\mathcal{L}_{CP} = -\frac{\alpha_S}{8\pi} \bar{\theta} \mathrm{Tr} G\tilde{G} \quad \rightarrow \quad \mathcal{L}_{CP} = -\frac{\alpha_S}{8\pi} \frac{a(x)}{f_a} \mathrm{Tr} G\tilde{G} \tag{9}$$

The potential (mass term) forces the field to its minimum where $\bar{\theta} = 0$.

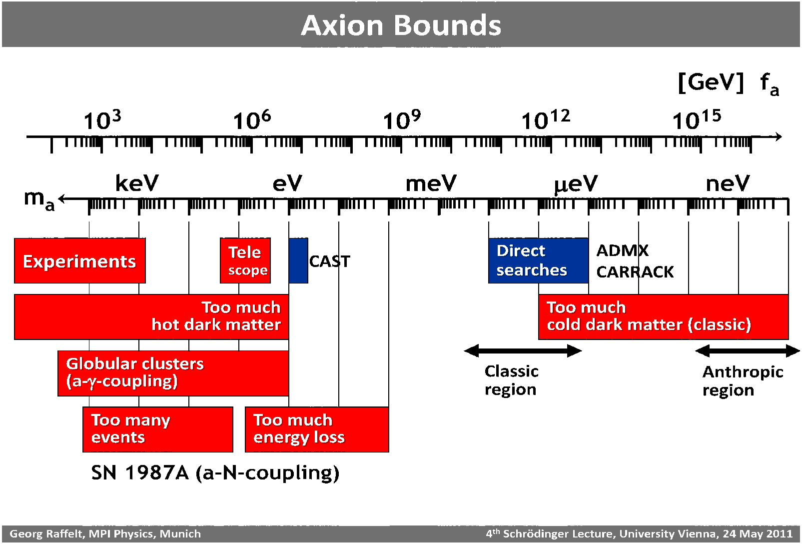

(from G. Raffelt)

Figure : The two diagrams contributing to the polarization tensor of baryonic matter, which defines the axial vector emissivity. The "normal" baryon propagators for particles (holes) are shown by single-arrowed lines directed from left to right (right to left). The double arrowed lines correspond to the "anomalous" propagators F (two incoming arrows) and F^{+} (two outgoing arrows).

The emissivity of this processes is given by

$$\epsilon_a = \frac{8}{3\pi} f_a^{-2}\, \nu(0)\, v_F^2\, T^5\, I_a, \qquad I_a = z^5 \int_1^\infty dy\, \frac{y^3}{\sqrt{y^2-1}} f_F\,(zy)^2\,, \tag{10}$$

$z = \Delta(T)/T$ and $f_F(x) = [1+\exp(x)]^{-1}$ is the Fermi distribution function. Note the different temperature dependence of the axion emissivity compared to that of the neutrino emissivity.

We now require that the axion luminosity does not exceed the neutrino luminosity

$$\frac{\epsilon_a}{\epsilon_\nu} = \frac{\alpha}{f_a^2 G_F^2 \Delta(T)^2} < 1, \tag{11}$$

where we set the ratio $I_a/I_\nu \simeq 1$ and find that $\alpha \simeq 73.7$ ($g_A = 1.25$). Our bound is given by (J. Keller and A. Sedrakian, Nucl. Phys. A, 897, 62, 2013)

$$\boxed{f_a > 7.4 \times 10^9 \text{ GeV} \left[\frac{0.1 \text{ MeV}}{\Delta(T)}\right],} \tag{12}$$

which translates into an upper bound on the axion mass

$$m_a = 0.62 \times 10^{-3} \text{ eV} \left(\frac{10^{10}\text{GeV}}{f_a}\right) \leq 0.84 \times 10^{-3} \text{ eV} \left[\frac{\Delta(T)}{0.1 \text{ MeV}}\right]. \tag{13}$$

The bound (12) can be written in terms of the critical temperature by noting that $\Delta(T) \simeq 3.06 T_c \sqrt{1 - T/T_c} \simeq T_c$ in the temperature range $0.5 \leq T/T_c < 1$ of most interest.

...but we can do better via full-scale cooling simulations

Axionic Cooling of Neutron Stars

In analogy to neutrinos in the case of S-wave the axion emissivity is given by

$$\epsilon^S_{aN} \quad = \quad \frac{2C_N^2}{3\pi} f_a^{-2}\, \nu_N(0)\, v_{FN}^2\, T^5\, I^S_{aN}, \quad I^S_{aN} = z_N^5 \int_1^\infty dy\, \frac{y^3}{\sqrt{y^2-1}} f_F\left(z_N y\right)^2, \quad (14)$$

where C_N are Peccei-Quinn charges for neutrons and protons (different T-behaviour!)

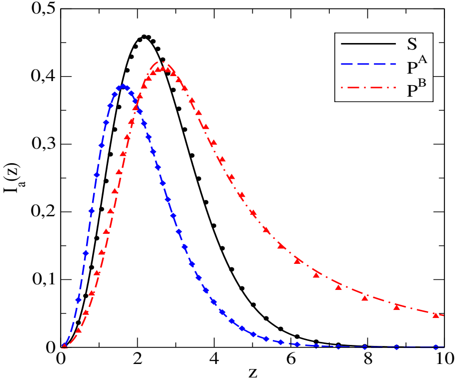

Figure : Dependence of the emissivity integrals on $z = \Delta(T)/T$. The exact results are shown by symbols, whereas the fits are shown by lines.

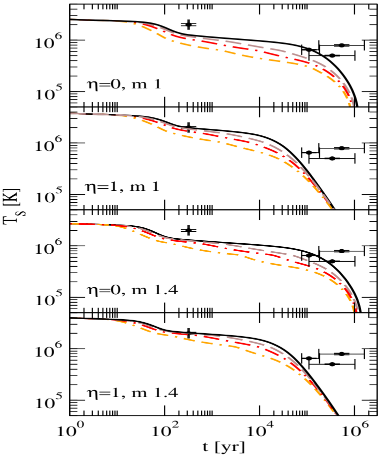

Figure : Cooling tracks (*redshifted* surface temperature vs age) for neutron star models with masses $m = 1$ and $m = 1.4$ (in solar units) for the cases of nonaccreted iron envelope ($\eta = 0$) and accreted light-element envelope ($\eta = 1$). The representative observational data includes (from left to right) the CCO in Cas A, PSR B0656+14, Geminga, and PSR B1055-52. Each panel contains cooling tracks for various values of the axion coupling constant; the case $f_a = \infty$ (solid line) corresponds to vanishing axion coupling – i.e., purely neutrino cooling. The axion cooling models are shown for the values $f_{a7} = 10$ (dashed), $f_{a7} = 5$ (dash-dotted), and $f_{a7} = 2$ (double-dash-dotted).

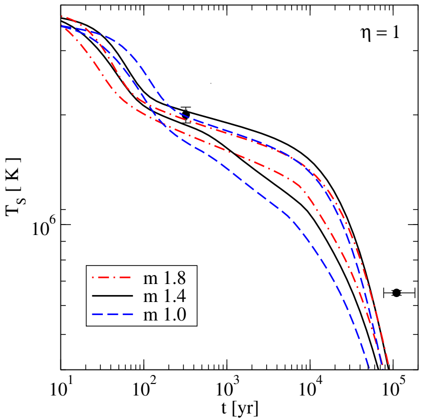

Figure : Cooling tracks of neutron star models with masses $m = 1$ (dash-dotted) 1.4 (solid) and 1.8 (dashed) for the case of an accreted light-element envelope ($\eta = 1$) along with the measured temperature of CCO in Cas A. For each value of mass, the upper curve corresponds to the cooling without axions, and the lower curve corresponds to axion cooling with $f_{a7} = 5$. Note the weak dependence on the surface temperature of models on the star mass.

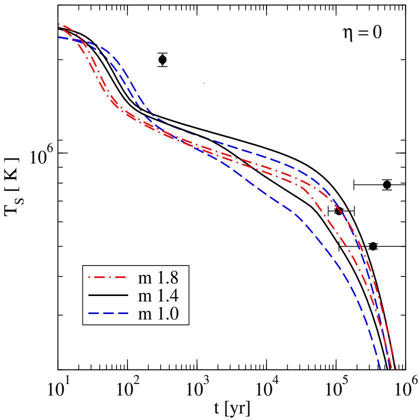

Figure : Cooling tracks of neutron star models with masses $m = 1$ (dashed) 1.4 (solid), and 1.8 (dash-dotted) for the case of a nonaccreted iron envelope ($\eta = 0$). The measured temperatures of PSR B0656+14, Geminga are consistent with neutrino cooling tracks; the uncertainty in the spin-down age of PSR B1055-52 and internal heating may account for marginal inconsistency. The axion cooling tracks are shown for $f_{a7} = 10$.

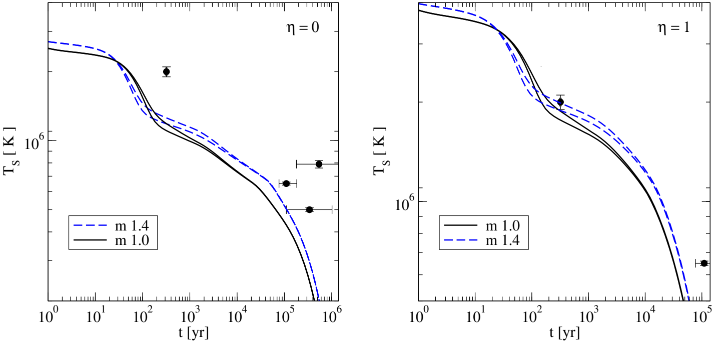

Figure : Cooling tracks of neutron star models with masses $m = 1$ (solid) and 1.4 (dashed) for the case of a nonaccreted iron envelope ($\eta = 0$) and accreted envelope ($\eta = 1$) and for $f_{a7} = 10$. For each mass, the two tracks differ by the value of the neutron PQ charge. The upper curves correspond to our standard choice $|C_n| = 0.04$, while the lower curves correspond to the case of enhanced axion emission with $|C_n| = |C_p| = 0.4$.

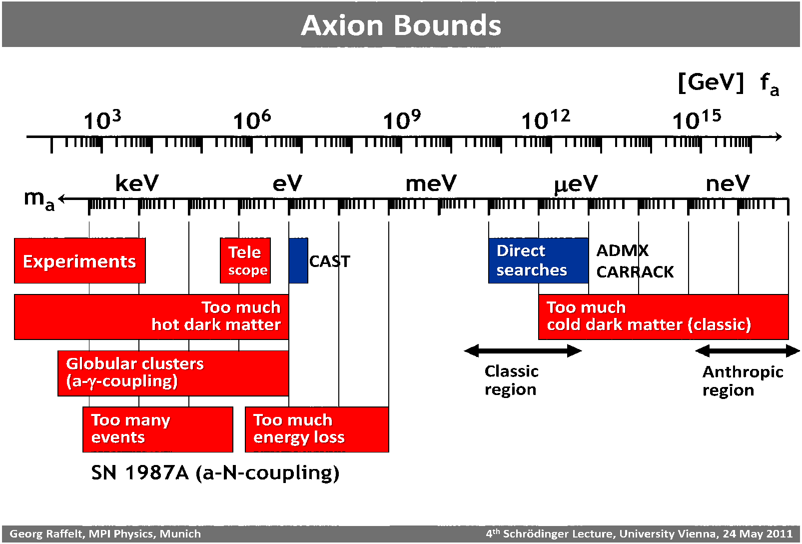

(from G. Raffelt)

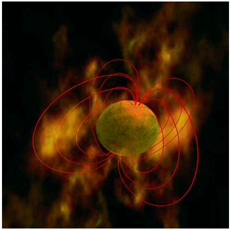

Unpairing effect in magnetars

- Coherence length of Cooper pairs

$$\xi_p \simeq \frac{\hbar^2 k_F}{\pi m^* \Delta} \gg \text{interparticle distance}$$

- Larmor radius:

$$R_L = \frac{cp_\perp}{eH}, \quad \text{for} \quad H \to \infty \quad R_L \to 0.$$

- Un-pairing sets in at a critical field H_{c2} when

$$R_L < \xi \quad \to \quad H_{c2} = \frac{\Phi_0}{2\pi\xi^2} \sim 10^{16}\,\mathrm{G}, \quad \Phi_0 = \frac{\pi\hbar c}{e}$$

- Because $H_{c2}(r) = H_{c2}(\rho)$:

$$\begin{aligned}
&\text{for} \quad H \leq \times 10^{15} \quad \text{fully s-conducting}\\
&\text{for} \quad H \geq 2\times 10^{16} \quad \text{completely non-s-conducting}\\
&\text{for} \quad 10^{15} \leq H \leq 2\times 10^{16} \quad \text{partially s-conducting}
\end{aligned}$$

Neutron ϕ and proton ψ condensate coupled to electromagnetism:

$$F[\phi,\psi] \quad = \quad F_n[\phi] + \alpha\tau|\psi|^2 + \frac{b}{2}|\psi|^4 + b'|\psi|^2|\phi|^2 + \frac{1}{4m_p}\left|\left(-i\hbar\boldsymbol{\nabla} - \frac{2e}{c}\boldsymbol{A}\right)\psi\right|^2 + \frac{B^2}{8\pi}$$

$$\delta F[\phi,\psi]/\delta\psi = 0, \quad \to \quad \frac{1}{4m_p}\left(-i\hbar\boldsymbol{\nabla} - \frac{2e}{c}\boldsymbol{A}\right)^2\psi + \alpha\tau\psi + b|\psi|^2\psi + b'|\phi|^2\psi = 0.$$

The equilibrium value of the condensate $\psi(\alpha\tau + b|\psi|^2 + b'|\phi|^2) = 0$, the two possible (normal-superconducting) equilibrium solutions

$$\psi = 0, \quad T > T_c, \qquad |\psi|^2 = -\frac{1}{b}(\alpha\tau + b'|\phi|^2), \quad T \le T_c.$$

The variation of the GL functional with respect to the electromagnetic vector potential $\delta F[\phi,\psi]/\delta\boldsymbol{A} = 0$ gives

$$\frac{c}{4\pi}\boldsymbol{\nabla}\times\boldsymbol{\nabla}\times\boldsymbol{A} = -\frac{i\hbar e}{m}\left(\psi^*\boldsymbol{\nabla}\psi - \psi\boldsymbol{\nabla}\psi^*\right) - \frac{4e^2}{mc}|\psi|^2(\boldsymbol{A}_{\rm em} + 2\boldsymbol{A}_{\rm ent}) = \vec{j}$$

The new aspect is the entrainment current $\propto \boldsymbol{A}_{\rm ent} \propto \boldsymbol{\nabla}\phi$.

For $H \to H_{c2}$ we have $\psi \to 0$ is small, therefore, linearize

$$\boldsymbol{\nabla} \times \boldsymbol{\nabla} \times \boldsymbol{A} = 0 + O(|\psi|^2).$$

$$\boldsymbol{\nabla} \times \boldsymbol{A}_{\rm ent} = 0,$$

except at the singular points where the neutron vortices are located. Therefore,

$$\boldsymbol{A} \to \boldsymbol{A}_{\rm em}$$

Consider the geometry

$$B \parallel z, \quad \boldsymbol{A}_{\rm em} = Bx \parallel y, \quad \psi = \psi(x).$$

The GL equation becomes

$$\boxed{-\psi'' + \frac{4\pi^2}{\Phi_0^2} B^2 x^2 \psi = -\frac{4m_p}{\hbar^2}\left(\alpha\tau + b'|\phi|^2\right)\psi + O(|\psi|^2).}$$

Solution in analogy to the harmonic oscillator:

$$-\frac{4m_p}{\hbar^2}\left(\alpha\tau + b'|\phi|^2\right) = \left(n + \frac{1}{2}\right)\frac{4\pi B}{\Phi_0}.$$

We are interested in the strongest field for which solutions with $\psi \neq 0$ are still possible, then case $n = 0$ corresponds $B = H_{c2}$.

$$H_{c2} = \frac{\Phi_0}{2\pi}\left[-\frac{4m_p}{\hbar^2}\left(\alpha\tau + b'|\phi|^2\right)\right] = \frac{\Phi_0}{2\pi\xi_p^2}\left[1 + \frac{|b'||\phi|^2}{\alpha|\tau|}\right], \quad (m_p|\alpha\tau|)^{1/2} = \frac{\hbar}{2\xi_p}.$$

The correction comes from Cooper-pair $\to$ Cooper pair scattering (from Alford, Good, Reddy, 2005)

$$\frac{b'|\phi|^2}{\alpha\tau} = \frac{n_n}{n_p}\frac{|b'|}{|b|}, \qquad \frac{n_n}{n_p}\frac{|b'|}{|b|} = \frac{27\pi^2}{8} G_{np}\frac{n_n^2}{\mu_p^2\mu_n^2}\frac{\Delta_p^2}{m_p k_{F_p}}.$$

n_b/n_0	k_{Fp}	Δ_p	m_p^*/m_p	ξ_p	δ_L	κ	H_{c2}
0.140	0.12	0.02	0.93	76.1	929.2	12.2	0.06
0.300	0.20	0.24	0.89	11.9	425.0	35.6	2.73
0.700	0.36	0.76	0.81	7.8	161.1	20.6	6.25
0.900	0.44	0.85	0.78	8.7	119.5	13.7	4.75
1.300	0.58	0.81	0.74	13.0	75.2	5.8	2.01
1.700	0.74	0.62	0.70	22.8	51.2	2.2	0.64
1.900	0.81	0.45	0.68	35.0	44.3	1.3	0.27
2.100	0.88	0.16	0.67	106.4	39.2	0.4	0.03

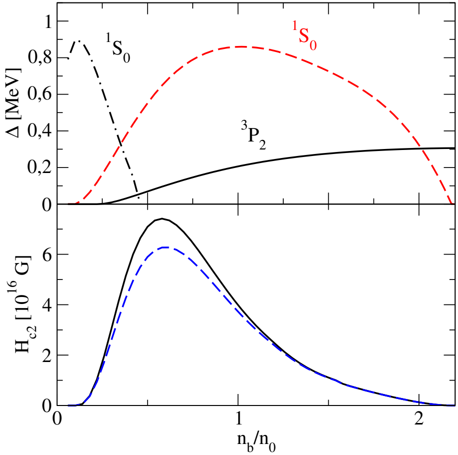

Figure : This H_{c2} takes into account the coupling the background neutron fluid in the framework of Ginzburg-Landau theory which gives 20% correction.

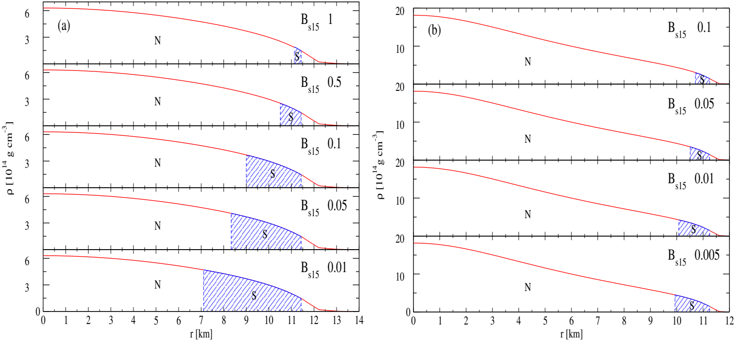

Left panel: $1.4M_\odot$ star internal structure with proton superconductor (shaded) core; right panel: the same for maximum mass star.

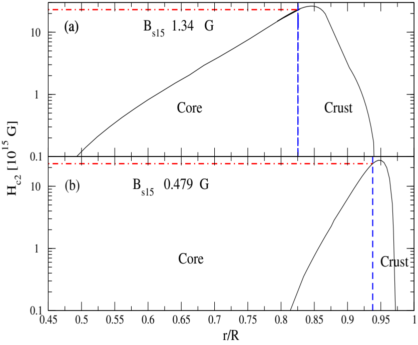

Dependence of H_{c2} on internal radius for (a) 1.4 $M_{\odot}$, $R = 13.85$ km star and (b) maximum-mass $2.67 M_{\odot}$, $R = 11.99$ km star. The crust core interface (vertical dashed line) is located at 11.43 km for the first star and at 11.25 km for the second. The maximal value of Hc2 in each model is attained at the crust-core interface. and is indicated by the horizontal dash-dotted line; the values of the corresponding surface fields are shown in the plot

Rotational dynamics

Low-field pulsars

$$electrons + \underbrace{proton - flux - tubes + neutron - vorticity}_{strongly\ coupled}$$

Scattering is electromagnetic Core is slowly responding to glitches producing part of post-glitch relaxation.

High-field pulsars

$$\underbrace{electrons + proton - plasma}_{strongly\ coupled} + neutron - vorticity$$

Strong force is at work (Sedrakian, Phys. Rev. D 58, 021301(R)).

Scattering of proton quasiparticles in the continuum off the cores of neutron vortices strongly temperature dependent

If protons are normal they couple to the neutron quasiparticles in the cores of neutron vortices via the strong force:

$$\tau^{-1} = 13.81 \times n_V \left(\frac{\mu_n}{\mu_p}\right)^2 \frac{T}{\varepsilon^0_{1/2}} \times e^{-\frac{\varepsilon^0_{1/2}}{T}} \frac{\hbar}{m_p^* \xi_n^2} \frac{d\sigma}{d\Omega}$$

Microscopic times-scales are of order of sec.

$$\eta = \frac{m_p^* n_p}{\tau_v n_V},$$

Drag-to-lift ratio and dynamical coupling time x

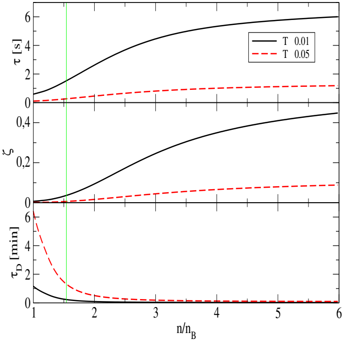

$$\zeta = \frac{\eta}{\rho_n \omega_0} = \frac{1}{2\Omega\tau_v} \frac{n_p}{n_n}, \qquad \tau_D = \frac{1}{2\Omega}\left(\zeta + \zeta^{-1}\right).$$

Our calculation indicates that magnetar cores, if unpaired, are coupled to the charged plasma of the star of dynamical coupling timescales of order of minutes at most.

Publications

1. A. Sedrakian,
Axion cooling of neutron stars.
Phys. Rev. D **93**, 065044 (2016). arXiv:1512.07828 [astro-ph.HE].

2. M. Sinha and A. Sedrakian,
Magnetar superconductivity versus magnetism: neutrino cooling processes.
Phys. Rev. C **91**, 035805 (2015). [arXiv:1502.02979 [astro-ph.HE]].

3. A. Sedrakian,
Rapid rotational crust-core relaxation in magnetars.
Astron. and Astrophys. **587**, L2 (2016). arXiv:1601.00056 [astro-ph.HE].